THE JOURNAL OF PHYSICAL CHEMISTRY B

ARTICLE

pubs.acs.org/JPCB

Protic Ionic Liquids Based on Decahydroisoquinoline: Lost Superfragility and Ionicity-Fragility Correlation

Kazuhide Ueno,[†] Zuofeng Zhao,[†] Masayoshi Watanabe,[‡] and C. Austen Angell*[,†]

[†]Department of Chemistry and Biochemistry, Arizona State University, Tempe, Arizona 85287-1604, United States

[‡]Department of Chemistry and Biotechnology, Yokohama National University, 79-5 Tokiwadai Hodogaya-ku, Yokohama 240-8501, Japan

Supporting Information

ABSTRACT: Physicochemical properties, ionicity, and fragility for protic ionic liquids (PILs) based on the protonation of the extremely fragile molecular liquid decahydroisoquinoline (DHiQ) by various Brønsted acids have been studied. The ionicity was evaluated using the Walden plot diagnostic, while the *m*-fragility (slope of T_g-scaled Arrhenius plot at T_g) was quantitatively measured by the Moynihan−Wang−Velikov variable scan rate, differential scanning calorimetry, method. DHiQ-derived PILs prove to cover the whole range of IL ionicities from poor IL to good IL, and even superionic, assessed from the Walden plot, depending on the choice of Brønsted acid. We find that the superfragile character of the parent DHiQ becomes completely suppressed upon conversion to ionic liquid, the initial value $m = 128$ sinking to $m = 45-91$ for the ionic liquid. Such values are in the intermediate to fragile range. The DHiQ-based PIL showing superionic behavior, anion [HSO_4^-], proves to be the case with the lowest *m* value ($m = 45$) so far reported for either aprotic or protic ILs. Both low fragility and dry proton conductivity can be attributed to an extended hydrogen bond network that is set up by the hydrogensulfate anion. The good DHiQ PILs have *m* values similar to those reported for typical aprotic ILs ($m = 60-80$), while the poor DHiQ PILs in which proton transfer from acid to base is weak show some memory of the parent fragility. Thus, a correlation of ionicity with *m*-fragility is characteristic of this system. A range of noncrystallizing, and also nonglassforming, behavior is observed in this series of compounds, suggesting a possible test for ideal glassformer existence.

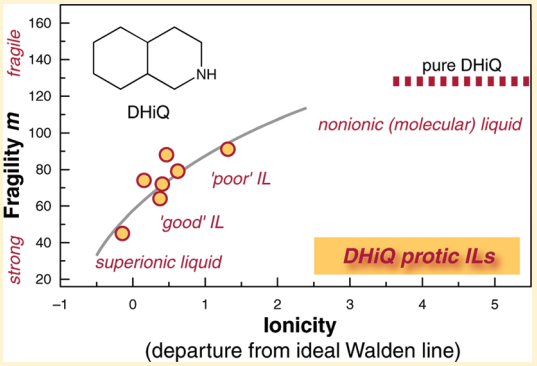

1. INTRODUCTION

The concept of fragility has been commonly employed for characterizing temperature-dependent dynamics of supercooled liquids near the glass transition.[1] On the basis of this concept, glass forming liquids can be classified according to where they fall between two extremes, the so-called strong/fragile pattern.[2] The *m*-fragility has been the most widely used metric for quantifying the fragility. The parameter *m* quantifies the deviation from Arrhenius law in the log *x* vs (T_g/T) plot and is defined as $m = \mathrm{d}\log x/\mathrm{d}(T_g/T)$ at T_g, where *x* is viscosity, the structural relaxation time, or frequently the dielectric relaxation time, and T_g is the glass transition temperature.[3,4] Strong liquids that show almost Arrhenius behavior have small *m* values ($m \approx 16$), while the fragile liquids, which display significant departures from Arrhenius behavior, have a larger *m* value. A limiting value near $m = 170$ has been projected.[5] In particular, Wang et al.[6,7] showed, by a thermal analysis of the hysteresis found characteristic of the glass transition, that for molecular liquids, the hysteresis tends to vanish when $m = 170$ so that the glass transition at that limit would resemble a second order thermodynamic transition. For polymers, there are a number of cases where $m > 170$, but for polymers, Sokolov has shown there are polymer-specific factors in operation.

The *m*-fragility has been determined for diverse glassformers including molecular, inorganic, ionic, metallic, and polymeric systems,[5,8] and many attempts have been made to find correlations with T_g itself[8] and with mechanical[9] and thermodynamic quantities such as the jump in heat capacity at T_g ($\Delta C_p(T_g)$),[10,11] excess entropy,[12] etc. However, there are always exceptions and much controversy remains about the origin of, and diversity in, the fragility of glassforming liquids.

Whereas the extreme strong cases in the strong/fragile pattern, such as SiO_2 and GeO_2, seem to have simple physics (conventional Arrhenius kinetics and little liquid excess heat capacity) and hence may seem of little interest; the extreme of high fragility is full of novelty. Fragile liquids have been extensively studied because of their unusual relaxation behavior. There is little agreement about what exactly makes a liquid fragile.

Among fragile molecular liquids, decahydroisoquinoline (DHiQ) rivals decalin for the role of the most fragile molecular liquid known so far. Both enthalpy relaxation[13] and dielectric relaxation[14] give the lead to decalin, with $m = 145$, but dielectric relaxation assigns

Received: September 7, 2011
Revised: November 28, 2011
Published: November 29, 2011

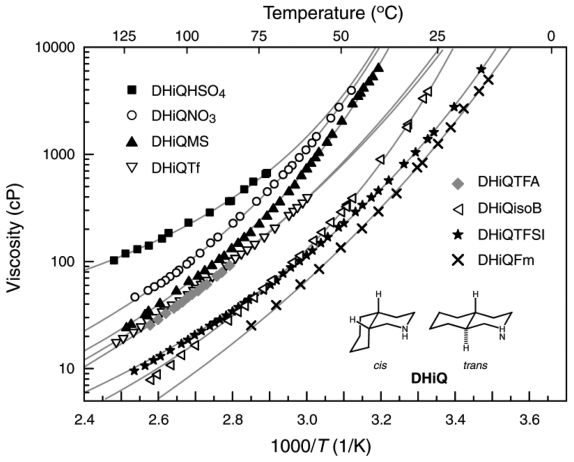

Figure 1. Temperature dependence of the viscosity for DHiQ PILs. The solid lines are based on best fitting to the VFT equation (eq 1).

DHiQ a higher value (m = 139) than does enthalpy relaxation (m = 128). Both are butterfly winged molecules (see inserts of Figure 1) and are characterized by unusually anharmonic vibrational densities of states in the quasilattice mode domain, according to neutron scattering studies.[15,16] Both have cis and trans isomers, which are mixed in the sources we use. These substances contrast strongly with the nonfragile behavior of the single-cycle paraffins like ethylcyclohexane.[17]

The basic nitrogen in one of the cycloalkane rings of the DHiQ molecule offers the possibility of forming derivative molecules or ions by simple chemical processes, such as Lewis acid adduct formation or protonation. The question of whether the fragility is enhanced or depressed by such modifications is an interesting one and forms the objective of the present study.

Protonation of DHiQ yields an ionic liquid in most cases, as the present report will document. Ionic liquids (ILs) are liquids composed solely of ions having melting points below 100 °C in the popular definition. They have received enormous attention in recent years, both as novel electrochemical systems,[18] as alternative solvents,[19] and most recently as biopreservatives and pharmacologically active agents of long shelf-life.[20] Largely because of the complex molecule-ion shapes, most ionic liquids are glass-formers. This is interesting since mixed cis−trans DHiQ itself has never been crystallized. Its hypothetical eutectic with a protic ionic liquid derivative is a good candidate for ideal glassformer (a substance that cannot crystallize because its glass temperature is higher than its melting point [or eutectic temperature, in the binary system case]).

A large number of studies on dynamic properties of the supercooled state and glass transition behavior of ILs have been carried out using dielectric spectroscopy,[21] heat capacity measurements,[22,23] dynamic mechanical measurements,[24] neutron scattering,[24] and conductivity measurements.[25] Xu et al.[26] studied qualitative fragilities of aprotic ionic liquids using the T_g-scaled Arrhenius plot of viscosity, and the fragility of the ILs was found to range from intermediate to very fragile, depending on the ionic structure. In a quantitative study of m-fragility for a series of n-alkylimidazolium tetrafluoroborate with different alkyl chain length, Leys and co-workers[27] reported that alkyl chain length had a little effect. Rather, the fragility was strongly influenced by Coulombic forces between cations and anions. This raises the possibility that the fragility of ILs correlates with an index for a dominant property of ILs, the ionicity, which is an indicator of how ideally ionic an IL is. Ionicity relates to the freedom of ions to carry their charge in response to electric field, i.e., to the degree of ionic dissociation.[28]

In the present study, we have focused on protic ionic liquids (PILs), which are a subclass of ionic liquids prepared by the transfer of protons from Brønsted acid to Brønsted base, and have studied the fragility of PILs based on the extremely fragile case of DHiQ. One of the particular interests of this work is to study how the superfragility of DHiQ changes on conversion to an ionic liquid. Unlike aprotic ILs, the ionicity (and thereby the physicochemical properties of PILs) varies significantly with the choice of combination of acid and base.[29−32] This wide range of tunability in the ionicity helps us to investigate the correlation between the ionicity and the fragility of the ILs from a broadened perspective.

To determine the ionicity of the DHiQ ILs, we first studied thermal properties, viscosity, and ionic conductivity for a series of DHiQ PILs prepared using different Brønsted acids. The ionicity has been assessed by a Walden plot approach,[26] while the m-fragility has been determined according to the variable scan rate differential scanning calorimetry protocol.[13] In a final section, we discuss the correlation between the ionicity and the m-fragility of DHiQ PILs with different ionic structures.

2. EXPERIMENTAL SECTION

2.1. Materials and Synthesis. Decahydroisoquinoline *cis*- and *trans*-mixtures (DHiQ, 98%) were purchased from TCI. Anhydrous formic acid (HFm, 98%) was obtained from Fluka. Nitric acid (68−70%, GR ACS grade) was obtained from EMD Chemicals Inc. Methane sulfonic acid (MS, 98+%), trifluoromethane sulfonic acid (HTf, 98+%), trifluoroacetic acid (HTFA, 99.5%), tetrafluoroboric acid (50% in water), and acetic acid (HAc, ACS grade) were obtained from Alfa Aesar. Trifluoromethanesulfonimide (HTFSI, 95%), sulfuric acid (99.999%), and isobutylic acid (HisoB, 99%) were obtained from Sigma-Aldrich. All chemicals were used as received.

The PILs were prepared, in all cases of this study, by neutralization reactions of the DHiQ base with anhydrous Brønsted acids. To prepare DHiQCl, HCl gas was passed through DHiQ dissolved in THF. The precipitated DHiQCl salt was filtered and washed with a large amount of THF, then dried under vacuum. For liquid Bronsted acids, stoichiometric amounts of the acid and DHiQ were mixed under a N_2 atmosphere while cooling in an ice bath. The reactions were carried out without any solvent. When necessary, the product was then heated above the respective melting point and stirred for several hours to ensure a complete reaction. The PILs based on strong acids, which have very low vapor pressures, were heated at 100 °C under vacuum to remove any excess of the more volatile acid or base along with any incidental water. In the case of the fluorinated anions (TFSI, Tf, and BF_4), the salts were purified in the manner typical for imdazolium-based aprotic ionic liquid preparations,[26] viz., extraction with dichloromethane/water followed by drying under vacuum at 100 °C. The resulting PILs were stored in a desiccator. For PILs based on weak acids, DHiQFm, DHiQAc, and DHiQisoB, were prepared by mixing the pure anhydrous acids stoichiometrically with DHiQ. In view of the relatively high component vapor pressures, no further drying purification was attempted as a precaution against stoichiometry change. For this group of PILs (from weak acids), freshly prepared samples were used for each measurement.

dx.doi.org/10.1021/jp2078727 |J. Phys. Chem. B 2012, 116, 63–70

2.2. Measurements. The thermal transitions, melting point (T_m), and glass transition temperature (T_g) were determined using a simple homemade DTA Instruments and refined using a differential scanning calorimeter (DSC-7, Perkin−Elmer). The DTA measurements were made as described in our previous work.[30] For DSC measurements, the instrument was calibrated prior to the measurements by the two-point method with indium (T_m = 156.6 °C) and cyclohexane (solid−solid transition, $T_{S1\rightarrow S2}$ = −86.6 °C) as the standard samples for high temperature and low temperature regions, respectively. Samples were sealed in aluminum pans and scanned at a rate of 20 K min^{-1} in a helium atmosphere.

Viscosity measurements were performed using a Brookfield cone−plate viscometer (RVTDCP, CP-40), which was calibrated at the company, and the accuracy was confirmed to 0.5% by measurement on a viscosity standard (Dow200). The temperature was controlled to 0.1 °C by means of a water circulating bath (LC20, Lauda) for lower temperatures and a heating oil bath for higher temperatures.

Ionic conductivities were measured by the standard complex impedance method, using a PARSTAT2273 (Princeton Applied Research) with a frequency range of 10 Hz to 1 MHz. The ionic liquids were contained in a dip-type cell with twin platinum electrodes. The cell constant of 0.59 cm^{-1} was determined using a 0.01 M KCl aqueous solution. The temperature was controlled to 0.1 °C by a Peltier temperature controller with an aluminum block.

Density values were measured with accuracy of ∼1% simply by measuring the weight of the sample filling a 1 mL volumetric flask at different temperatures. Before each measurement, the flask was maintained in an aluminum block at the desired temperature for half an hour to obtain a uniform temperature.

The *m*-fragilities of the PILs were determined by the Wang−Velikov variable cooling rate-constant heating rate fictive temperature method[13] using the calibrated DSC-7. A series of heat flow measurements were performed over the temperature range T_g − 50 °C to T_g + 30 °C. To obtain the difference between the supercooled liquids and glassy states in the standard scan (ΔC_p), heat capacity measurements were also made using a sapphire standard.

3. RESULTS AND DISCUSSION

Our objective in this section is to show how the fragility of the DHiQ is systematically lost as it is converted to a cationic form by protonation and how this loss of fragility is correlated with the ionicity of the ionic liquid that is formed (and which itself is determined by the free energy drive behind the proton transfer). To achieve this, we first present, in sections 3.1−3.3, characterization data for the new ionic liquids, particularly viscosity and conductivity data, which we use in section 3.4 to obtain the ionicity but that cannot themselves provide reliable estimations of the fragilities. The fragilities are instead obtained using the Wang−Velikov scanning calorimetry method, which reliably yields the Arrhenius slope for relaxation at the glass transition. These results are described in section 3.5, and finally their relation to ionicity is examined and discussed in section 3.6.

3.1. Thermal Properties. Melting point (T_m) and glass temperature (T_g) of DHiQ protic ionic liquids (DHiQ PILs) and the parent DHiQ are summarized in Table 1. The final column of Table 1 also includes the difference in pK_a values for the Brønsted acid−base combination (ΔpK_a), where ΔpK_a = pK_a(base) − pK_a(acid), based on aqueous solution measurements

Table 1. Glass Transition Temperature (T_g) and Melting Point (T_m) at a Scan Rate of 20 K/min, Difference in pK_a between Acid and Base (ΔpK_a), and T_g/T_m Ratio for DHiQ PILs[a]

ionic liquid	T_g (K)	T_m (K)	T_g/T_m	ΔpK_a
DHiQTf	237	331	0.72	25.2
DHiQTFSI	227	n.d.		23.2
DHiQCl	n.d.	442		18
DHiQHSO$_4$	246	340	0.72	14
DHiQNO$_3$	238	338	0.70	12.4
DHiQMS	228	328	0.70	11.6
DHiQTFA	232	340	0.68	11.3
DHiQBF$_4$	n.d.	353		10.5[b]
DHiQFm	212	n.d.		7.25
DHiQAc	n.d.	351		6.25
DHiQisoB	226	n.d.		6.16
DHiQ (base)	178	n.d.		0

[a] pK_a values for Brønsted acids and DHiQ were obtained from refs 33 and 34, respectively; n.d., not detected. [b] The pK_a value for HBF$_4$ is controversial.

and p*K*a values for the acids and DHiQ, which were obtained from the literature.[33,34] Except for the chloride case, DHiQ-based PILs have T_m lower than 100 °C and thereby qualify as ionic liquids in the currently popular usage.

Except for three cases (DHiQCl, DHiQBF$_4$, and DHiQAc, which showed only the endothermic melting peak), the salts all showed well-defined glass transitions, characterized by the heat capacity changes observed in DSC thermograms. No melting endotherm at all was observed for the cases DHiQTFSI, DHiQFm, and DHiQisoB at a scan rate of 20 K min^{-1}. Such good glassforming properties may have their origin in the same molecular shape factor that, in combination with the cis−trans complexity, has made DHiQ itself impossible to crystallize so far. The values of T_g/T_m, where both could be measured, are given in the table and, as expected by tautology, are not far from the 2/3 rule expectation. Those that would likely violate the rule are excluded by the absence of either (i) a measurable T_g (in the two high-melting cases for which T_g/T_m would be ≪2/3) or (ii) an absence of a measurable T_m in the three cases where only T_g was recorded (T_g/T_m would be ≫2/3). The latter of course are the more interesting, as we discuss in the Conclusions section, related to the ideal glassformer conjecture.

3.2. Viscosity. DHiQ-based PILs are quite viscous liquids at room temperature with viscosities falling in the range 100−3000 cP at 50 °C depending on the ionic structure. The data are displayed in Figure 1. The viscosities follow the order HSO$_4$ > NO$_3$ > MS > Tf > TFA > TFSI ≈ isoB > Fm. Although the viscosities of ILs are determined by a complex interplay between electrostatic, van der Waals, and hydrogen-bonding forces, one might expect the electrostatic interaction between ions created by the proton transfer to be the dominant factor. However, the expectation that the Tf and TFSI salts (those with largest ΔpK_a values) would then be the most viscous of the series is not borne out, nor do these salts have the highest values of T_g, which are often taken as a measure of the cohesive energy. The expectation that the PILs with the smallest proton transfer energy should have the lowest T_g values and the lowest viscosities is borne out, and this is consistent with the conductivity−viscosity relationships to be discussed below. High viscosities in the series are related to the

dx.doi.org/10.1021/jp2078727 |J. Phys. Chem. B 2012, 116, 63–70

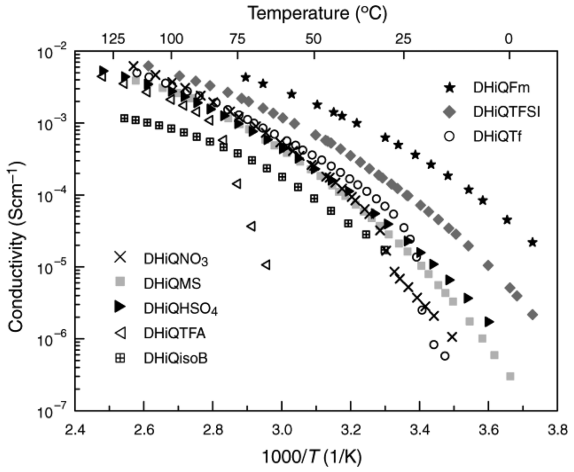

Figure 2. Temperature dependence of ionic conductivity for DHiQ PILs.

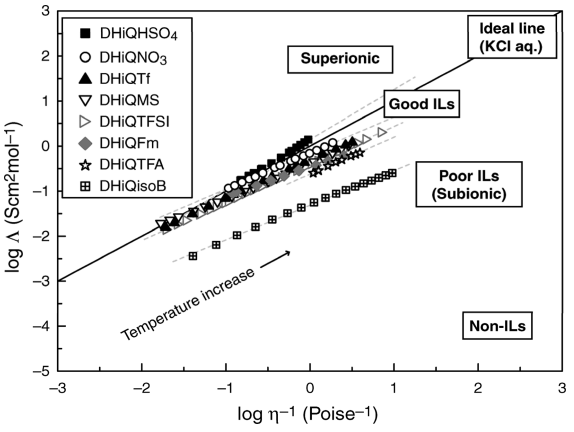

Figure 3. Walden plot for DHiQ PILs, which include the classification of ioncity in ILs. The solid line indicates the ideal line for a completely dissociated electrolyte aqueous solution (KCl aq), and the dotted lines are linear fits to the data.

ability to form an interparticle hydrogen bond network. Overall, there is good agreement between the order of viscosity and the order of T_g, which is only expected if the spread of fragilities is not too great. Why the nitrate, with its intermediate basicity, should be the case with highest viscosity, and T_g, except for bisulfate, is not at all clear.

Ambient temperature viscosity is determined by a combination of glass temperature and the rate at which the viscosity changes with temperature above T_g, i.e., the fragility of the liquid. With respect to fragility, the series of DHiQ PILs covers a wide range of possible values like the alkylammonium-based PILs that were reported previously.[30] The fragility is often obtained from the fit of the data to the Vogel−Fulcher−Tammann (VFT) equation[35−37] for η written as

$$\eta = \eta_0 \exp[B/(T - T_0)] = \eta_0 \exp[DT_0/(T - T_0)] \quad (1)$$

where η_0, B, D, and T_0 are adjustable parameters, and small D indicates large fragility. However, this is often misleading if the range of viscosities being fitted is far above T_g, frequently yielding T_0 values higher than T_g, which is unphysical. The more reliable measure is the m-fragility determined from the slope of the T_g-scaled Arrhenius plot for viscosity ($m = \mathrm{d}\log\eta/\mathrm{d}(T_g/T)$ at T_g) = $E_\eta/2.303RT_g$ from the VFT equation, using data near T_g, or simply the relationship $m = 16 + 590/D$, which assumes a value of 10^{-4} poise for η_0.[38] For instance, Shamim and Mckenna studied the m-fragility of alkylimidazolium aprotic ionic liquids using the VFT parameters obtained from their accurate dynamic viscosity measurement near T_g.[39] For most laboratories, viscosity measurements near T_g are difficult to make with accuracy, but a simple DSC technique gives equally reliable data and has been used by us to decide, in the later discussion, the manner in which the superfragility of the parent DHiQ has been lost in the conversion to an ionic form (and equally so on conversion to a covalently bound molecular form).

Our viscosity data, in summary, are important mainly for the assessment of the ionicity, that we describe in section 3.4 and then correlate with the fragility in section 3.5.

3.3. Ionic Conductivity. The ionic conductivities of the PILs of this study are presented as Arrhenius functions of temperature in Figure 2. The ionic conductivity is determined jointly by the mobility of the charge carriers and their number density (concentration). As might be expected from their higher viscosities (i.e., slower moving particles), DHiQ PILs are relatively poor ionic conductors. The conductivity values are more than 1 order of magnitude lower than those for ammonium-based PILs[30] at room temperature. For the same reason, the DHiQFm and TFSI, having lower viscosities, exhibit the highest conductivities of the PILs studied here. However, the low conductivity of DHiQisoB is found in the face of a relatively low viscosity. The reason for this lies in the lower ionic concentration caused by the incomplete proton transfer (lower ΔpK_a) in this PIL as the Walden plot below will clearly show.

Like the viscosity, the conductivity of DHiQ PILs in their liquid range can be fitted by the VTF equation for conductivity, $\sigma = \sigma_0 \exp[DT_0/(T-T_0)]$. Indeed, for aqueous solutions it is commonly found that the T_0 parameter is identical within the fitting uncertainty for the two properties (conductivity and viscosity). However, the D value is always smaller for conductivity, so the fragility assessed in this way is disconcertingly smaller. In less dissociating solvents than water, quite misleading fragility information would be obtained due to a temperature-dependent degree of association that is not taken into account by the simple VFT equation. This is also the case when ionicity is low.

3.4. Ionicity. The ionicity of an IL can be defined as the degree to which a liquid, comprised of charged particles, behaves as a collection of completely free ions, each surrounded by a uniform density of ions of the opposite charge. Such a collection becomes stabilized, relative to the energy of a collection of ion pairs, by the amorphous equivalent of a crystal Madelung (free) energy, which is the origin of the low vapor pressure for which ILs are famous. There are different techniques being used to assess the ionicity of ILs, including (i) the comparison of ionic mobility with viscosity using a Walden plot,[26,40] (ii) the molar conductivity ratio obtained from measured diffusivities via the Nernst−Einstein equation and by direct measurement,[41] and (iii) a potentiometric titration method.[42] The Walden plot approach, based on plots of log(equivalent conductivity, Λ) versus log(reciprocal of viscosity, η^{-1}), is a facile and versatile method applicable to any kind of IL. The molar conductivity ratio method, much used by one of us (M.W.), is most useful for high ionicity cases. We note that, for aprotic ILs, the ionicity determined by the measured-to-calculated (diffusivity-based) molar conductivity ratio method has been shown to be well correlated with the deviation from the ideal Walden line.[28]

dx.doi.org/10.1021/jp2078727 |J. Phys. Chem. B 2012, 116, 63–70

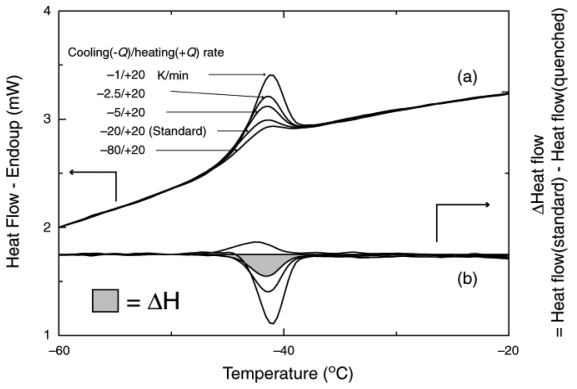

Figure 4. (a) DSC upscans at the heating rate of 20 K/min, of DHiQTFSI quenched with different cooling rates, where the −20/+20 K/min curve is called the standard scan. (b) Difference in the heat flow between the standard curves and the others, where the integral of the shaded region gives the excess enthalpy of the quenched glasses, and is used to find the difference in fictive temperatures.

The reference straight line in the Walden plot represents the behavior of fully dissociated electrolytes of small particles and can be calibrated using data for dilute aqueous KCl solutions in which the motion of each ion is controlled by the viscous forces in the solution. The ionicity can be characterized in terms of adherence to the ideal behavior in the Walden plot (ionicity = unity), and accordingly, ILs can be classified as superionic, good IL, poor IL, and nonionic (molecular) liquid as in Figure 3.[26] An IL whose Walden plot falls an order of magnitude below the ideal line can be assigned an ionicity of 0.1.

Data for the present DHiQ PILs are presented in Figure 3. For DHiQ PILs based on strong acids, the data lie only slightly below the ideal line (i.e., in the good IL domain), whereas DHiQisoB (with the lowest ΔpK_a in Table 1) shows a large deviation, so it can be classified as a poor IL. At higher temperatures, the deviation becomes larger in most DHiQ ILs, which we attribute to the temperature-induced ionic association[29] discussed in the previous section.

The deviation from the ideal Walden line is, however, not reliably correlated (inversely) with the value of ΔpK_a (aqueous). For instance, trifluoroacetic acid is a much stronger acid than formic acid (ΔpK_a of 11.3 for DHiQTFA and 7.25 for DHiQFm), but the Walden plot deviation, ΔW, for DHiQFm is smaller than that for DHiQTFA. This may be due to the role in dissociation played by the high Lewis basicity for TFA^- reported by Mudring et al. in their study on anion Lewis basicity of ILs using a Ni-based indicator complex.[43]

For $DHiQHSO_4$, the data lie above the ideal Walden line in the superionic region, and the slope of the plot is greater than unity. Similar superionic behavior has already been observed for pyrrolidinium HSO_4[44] and for some dihydrogen phosphates. This indicates a contribution to conductivity by some mechanism other than the common vehicular process, presumably proton-hopping or Grotthuss-type transport.[45]

Evidently the ionicity for the DHiQ PILs studied here can cover all classes of ILs, from poor IL to good IL, and even to superionic, depending on the Brønsted acid that protonates the DHiQ. Such a broad range of ionicity offers the possibility of investigating the correlation between ionicity and fragility for DHiQ PILs.

3.5. *m*-Fragility. To determine the *m*-fragilities for DHiQ PILs through T_g, we adopted the variable scan rate DSC-based protocol developed by Wang et al.[13] In their systematic study of a group of molecular liquids with diverse character ($50 < m < 150$), the *m*-fragilities obtained mostly agree well with those from dielectric relaxation, heat capacity spectroscopy, and viscosity studies. A similar calorimetric method was used by Moura-Ramos and co-workers[46] to study aprotic ILs, finding *m*-fragilities of two methoxyethoxyethyl-substituted imidazolium ionic liquids (m = 49 for Cl and 51 for PF_6). Here, we briefly review the Wang et al. procedure (see ref 13 for details).

In Figure 4, we depict typical raw data (DHiQTFSI), showing standard upscans ($Q^+ = 20$ K min^{-1}) for samples that had been cooled at different controlled rates ($Q^- = 1-80$ K min^{-1}) and (lower curves) the differences between the standard rate scan and other scans. The differences, converted to enthalpies (ΔH in Figure 4), are used to obtain the fictive temperatures of the nonstandard scan samples using the approximate relationship

$$T_f = T_f^s + \frac{\Delta H(Q)}{\Delta C_p} \quad (2)$$

where T_f^s is the original Moynihan fictive temperature,[47] and ΔC_p is the difference in heat capacity between supercooled liquids and glassy states measured in the standard scan at T_f^s. The standard

Table 2. Data Used in Obtaining the *m*-Fragility by the Wang–Velikov Method, Glass Transition Temperature (T_g), Fictive Temperature of Standard Upscan (T_f^s), Difference in Heat Capacity between Glassy and Supercooled Liquid States Determined at T_f^s (ΔC_p), and Resulting *m*-Fragility for DHiQ PILs[a]

ionic liquid	T_g (K)	T_f^s (°C)	ΔC_p (J/g K)	m
DHiQ (base)	178	181	0.84	128
DHiQTf	237	237	0.34	
DHiQTFSI	227	227	0.25	72
$DHiQHSO_4$	246	249	0.36	45
DHiQMS	228	227	0.41	64
$DHiQNO_3$	238	238	0.36	74
DHiQTFA	232	233	0.30	79
DHiQFm	212	213	0.46	88
DHiQisoB	226	226	0.56	91

[a] Data of DHiQ (base) is obtained from ref 13.

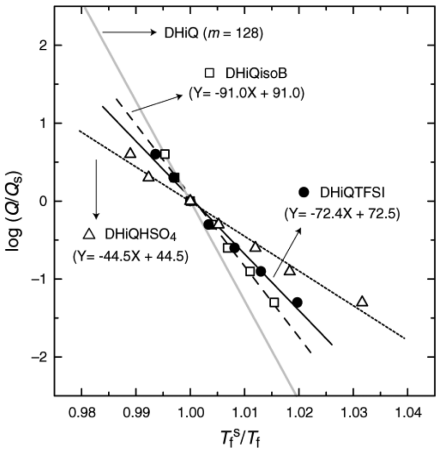

Figure 5. Scaled Arrhenius plots of the cooling rate vs the resulting fictive temperature from eq 2, for three DHiQ PILs.

dx.doi.org/10.1021/jp2078727 |J. Phys. Chem. B 2012, 116, 63–70

fictive temperature T_f^s and the heat capacity jump ΔC_p for DHiQ PILs are listed in Table 2. Then, the *m*-fragility can be obtained directly from the slope (or the intercept) of the reduced cooling rate versus reciprocal reduced fictive temperature (Figure 5) using the simple expression

$$\log\left(\frac{Q}{Q_S}\right) = m - m\frac{T_f^S}{T_f} \quad (3)$$

The advantage of this method is that the fictive temperatures are obtained more precisely than the glass temperatures T_g used in alternative DSC determinations of the activation energy for enthalpy relaxation because they do not depend on T_g-defining constructions in the domain of rapid (nonequilibrium) change in apparent heat capacity (which would invalidate data from 40 and 80 K/min scans).

The *m*-fragilities of DHiQ PILs are collected in Table 2 along with T_g, T_f^s, and ΔC_p values. We did not determine the *m*-fragility of DHiQTf because crystallization occurred during slow cooling scans ($Q < 5$ K min^{-1}). Clearly, the *m*-fragility for all DHiQ PILs are much lower than that for DHiQ itself (m = 128−139 depending on method of determination), indicating again that superfragility of DHiQ has disappeared on conversion to the ionic liquid. The fragilities are seen to vary from intermediate to fragile depending on the ionic structure.

The value of *m*-fragility for DHiQ PILs derived from strong acids ranged from 64 to 79 except for $DHiQHSO_4$. Similar *m* values have been reported for aprotic ILs: m = 71 for 1-hexyl-3-methylimidazolium TFSI,[24] m values between 73 and 80 for alkylimidazolium ILs with different anions,[39] and m values between 55 and 78 for *n*-alkylimidazolium BF_4 with different alkyl chain lengths.[25,27] Various authors have categorized protic ILs into intermediate to fragile liquid using T_g-scaled Arrhenius plots,[30,31,44] but quantitative estimates of the fragility have been rather limited.[48,49]

The fragility of superionic $DHiQHSO_4$ (m = 45) is at the low end of the fragility range reported for aprotic and protic ILs. Since HSO_4 anion has both proton accepting and donating sites, it is capable of linking up to form a hydrogen bond network. The higher viscosity and Grotthuss-type superionic transport evidently result from the existence of this network. Similar and smaller *m* values are commonly seen in inorganic network glass formers (e.g., m = 32 for B_2O_3) and hydrogen bond network glass formers (e.g., m = 40 for *n*-propanol).[38]

The fragilities of the remaining cases are best discussed in the context of the ionicities deduced from the Walden plot above.

3.6. Correlation of *m*-Fragility with Ionicity. DHiQ PILs formed from weak acids (DHiQFm and DHiQisoB) are more fragile than the others. Although NMR studies have found that only single (average) proton NMR resonances (i.e., no separate cation and molecular acid peaks) are found in PILs of smaller ΔpK_a values, the average signals do reflect a different proton environment for these PILs. The weaker proton transfer is manifested in a less shielded (more downfield) chemical shift. The weaker the transfer, the more the fragile DHiQ character can be thought of as remaining.

To quantify the fragility-ionicity relationship, we show, in Figure 6, the measured fragilities as functions of two measures of ionicity, (a) ΔpK_a and (b) the deviation, at log η^{-1} = 0, from ideal Walden behavior, ΔW. In Figure 6a, we assign pure DHiQ in which there is no proton transfer, a ΔpK_a value of zero. In

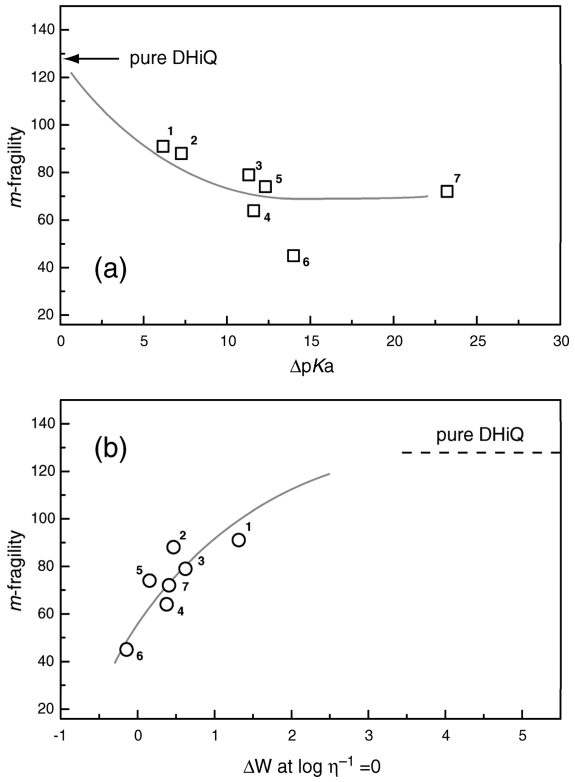

Figure 6. Correlation between the *m*-fragility and the ionicity; (a) ΔpK_a and (b) ΔW at log η^{-1} = 0 in the Walden plot (Figure 3). Data for parent DHiQ are represented by the arrow in panel a and dashed line in panel b. 1, DHiQisoB; 2, DHiQFm; 3, DHiQTFA; 4, DHiQMS; 5, $DHiQNO_3$; 6, $DHiQHSO_4$; and 7, DHiQTFSI. The solid lines in the plots are guides to the eye. Note that the correlation of fragility with the internally measured quantity ΔW is better than that with the external quantity ΔpK_a from aqueous data.

Figure 6b, there is a problem in assigning a specific point to pure DHiQ as it is a molecular liquid (non-IL). It has no meaningful deviation from the Walden line, unless we suppose some small conductivity due to self-dissociation by proton exchange between amine groups. In the latter case, the ΔW could exist and would obviously be large, so we can use the pure DHiQ fragility as a limit (dashed horizontal line) in the Figure 6b plot. While *m* versus ΔpK_a (Figure 6a) fails to correlate data for superionic $DHiQHSO_4$, a good correlation, which includes $DHiQHSO_4$ as well as DHiQTFSI, is found in *m* versus ΔW (Figure 6b).

The question of distinct species in the poor ILs is an important one. It could be clarified by an experiment of time scale shorter than that of proton NMR, for instance, the IR vibrational mode spectra (seeking both N^+−H and H−[Anion]), but to our knowledge this remains to be carried out. In the meantime, we can carry out a further experiment in which the fragilities of solutions of a good PIL containing an excess of DHiQ are determined. Results of such a study are shown in Figure 7. The mixture is that of DHiQ and the nonfragile PIL, DHiQMS, m = 64 (Table 2).

It is seen that, while the T_g values vary nonlinearly with mole fraction, the values of fragility changes smoothly between the two extremes. The *m*-fragility of the least ionic PIL of Table 2, namely, DHiQisoB, m = 91, is obtained in a mixture with about 17% excess (free) DHiQ, which is qualitatively consistent with

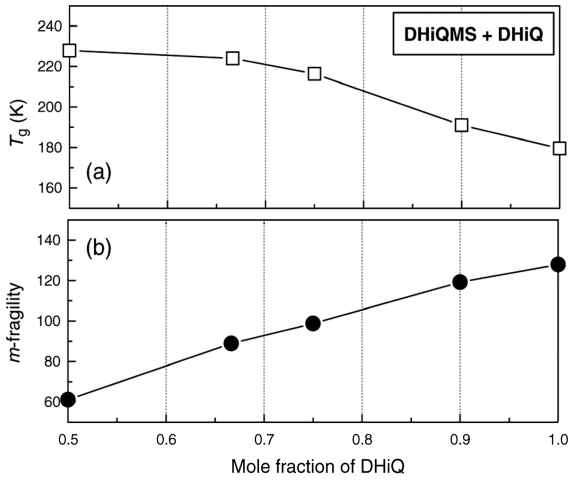

Figure 7. (a) T_g and (b) *m*-fragility plotted as a function of mole fraction of DHiQ in DHiQMS−DHiQ mixtures.

the ionicity of 0.1 (effectively 10% free DHiQ) that would be assigned to DHiQisoB from the Walden plot deviation.

4. CONCLUSIONS

Through the study on ionicity and the quantitative estimation of fragility, we found that the superfragility of DHiQ diminishes when Columbic forces are introduced and that the fragility of the proton-transfer ionic liquid is well correlated with the ionicity (ΔpK_a, ΔW) of the PIL: the *m*-fragility decreases as the ionicity increase. As with glass-forming liquids that possess a network structure, PILs that can set up a hydrogen-bonded network have low to intermediate fragility and the networking protons prove to have hopping dynamics that confers superionic (superprotonic) character.

Finally we must ask, with what other properties of DHiQ can we correlate the remarkably high fragility that is taken away so dramatically on strong protonation. An outstanding characteristic of both decalin[15] and DHiQ[16] is the anharmonicity of the low frequency (quasi-lattice) vibrational modes. Even in the glassy state, the increase of temperature has a powerful effect on the observed low frequency spectrum. Obviously it would be interesting to see if this unusual behavior of the vibrational modes disappears on protonation to the ionic liquid state since vibrational anharmonicity has often been linked to fragility.[50]

We make a concluding observation related to the unobservability of crystallization in cis−trans mixtures of DHiQ and in some of its PILs. The observation relates to the question of ideal glassformers,which are liquids that pass into the glassy state without ever becoming supercooled with respect to some crystal or combination of crystals.[51]

The failure to observe any crystallization at all implies that the glass temperatures of both DHiQ and, for instance, DHiQTFSI, must be not only greater than $2/3T_m$ but also greater than $3/4T_m$, which is the limit for observability of crystallization. The question is whether the decrease in melting points that accompanies mixing with other components that are insoluble in the other's crystal lattices, will be enough to push the eutectic temperatures below the glass temperature. In other words, can the eutectic lie more than 25% below the melting point? After all, cases of nonideal solutions are known in which the eutectic falls as much as 50% below the lowest component melting point (Au−Si for instance).

Obviously and unfortunately, this will be impossible to decide by direct measurements. However, the liquidus of the system $[DHiQ^+][Tf^-]$ + DHiQ could be easily determined because the triflate is high-melting. Then, it would be interesting to observe the course of this liquidus in relation to the (measurable) T_g values of the binary solutions. How quickly is it approaching T_g? One could then suppose that the TFSI-DHiQ system would have the same liquidus slope since the chemistry of the solution interactions would be similar to that of the Tf-based system. Since the T_g vs composition relationship would be similar in each case (which could be checked), it would be easy to judge if the interesting but unmeasurable liquidus for the TFSI-based system would penetrate the T_g locus or not (assuming a maximum pure component melting point of $1.33T_g$).

■ ASSOCIATED CONTENT

Supporting Information. Anharmonicity of quasi-lattice modes in glass and superfragile liquid states of of decahydroisoqinoline. This material is available free of charge via the Internet at http://pubs.acs.org.

■ AUTHOR INFORMATION

Corresponding Author

*Tel: (480) 965-7217. Fax: (480) 965-2747. E-mail: caa@asu.edu.

■ ACKNOWLEDGMENT

K.U. acknowledges financial supports (research fellowship for young scientists and excellent young researchers, overseas visit program) provided by JSPS.

■ REFERENCES

(1) Angell, C. A. *J. Non-Cryst. Solids* **1985**, *73*, 1–17.
(2) Angell, C. A. In *Relaxations in Complex Systems*; Ngai, K. L., Wright, G. B., Eds.; NRL: Washington D. C., 1985; p 3.
(3) Plazek, D. J.; Ngai, K. L. *Macromolecules* **1991**, *24*, 1222–1224.
(4) Böhmer, R.; Angell, C. A. *Phys. Rev. B* **1992**, *45*, 10091–10094.
(5) Wang, L.-M.; Angell, C. A.; Richert, R. *J. Chem. Phys.* **2006**, *125*, 074506.
(6) Wang, L.-M. *J. Phys. Chem. B* **2009**, *113*, 5168–5171.
(7) Wang, L.-M.; Mauro, J. C. *J. Chem. Phys.* **2011**, *134*, 044522.
(8) Qin, Q.; McKenna, G. B. *J. Non-Cryst. Solids* **2006**, *352*, 2977–2985 and references therein.
(9) Novikov, V. N.; Sokolov, A. P. *Nature* **2004**, *431*, 961–963.
(10) Huang, D.; McKenna, G. B. *J. Chem. Phys.* **2001**, *114*, 5621–5630.
(11) Angell, C. A. *Science* **1995**, *267*, 1924–1935.
(12) Martinez, L.-M.; Angell, C. A. *Nature* **2001**, *410*, 663–667.
(13) Wang, L.-M.; Velikov, V.; Angell, C. A. *J. Chem. Phys.* **2002**, *117*, 10184.
(14) Richert, R.; Duvvuri, K.; Duong, L. T. *J. Chem. Phys.* **2003**, *118*, 1828.
(15) Plazanet, M.; Schober, H. *Phys. Chem. Chem. Phys.* **2008**, *10*, 5723–5729.
(16) Plazanet, M.; Schober, H.; Angell, C. A. See Supporting Information.
(17) Mandanici, A.; Huang, W.; Cutroni, M.; Richert, R. *J. Chem. Phys.* **2008**, *128*, 124505.
(18) Galinski, M.; Lewandowski, A.; Stepniak, I. *Electrochim. Acta* **2006**, *51*, 5567–5580.

(19) Wasserscheid, P.; Keim, W. *Angew. Chem., Int. Ed.* **2000**, *39*, 3772–3789.
(20) Byrne, N.; Angell, C. A. *J. Mol. Biol.* **2008**, *378*, 707–714.
(21) Ito, N.; Huang, W.; Richert, R. *J Phys. Chem. B* **2006**, *110*, 4371–4377.
(22) Yamamuro, O.; Minamimoto, Y.; Inamura, Y.; Hayashi, S.; Hamaguchi, H. *Chem. Phys. Lett.* **2006**, *423*, 371–375.
(23) Shimizu, Y.; Ohte, Y.; Yamamura, Y.; Saito, K.; Atake, T. *J. Phys. Chem. B* **2006**, *110*, 13970–13975.
(24) Russina, O.; Beiner, M.; Pappas, C.; Russina, M.; Arrighi, V.; Unruh, T.; Mullan, C. L.; Hardacre, C.; Triolo, A. *J. Phys. Chem. B* **2009**, *113*, 8469–8674.
(25) Leys, J.; Rajesh, R. N.; Menon, P. C.; Glorieux, C.; Longuemart, S.; Nockemann, P.; Pellens, M.; Binnemans, K. *J. Chem. Phys.* **2010**, *133*, 034503.
(26) Xu, W.; Cooper, E. I.; Angell, C. A. *J. Phys. Chem. B* **2003**, *107*, 6170–6178.
(27) Leys, J.; Wübbenhorst, M.; Menon, C. P.; Rajesh, R.; Thoen, J.; Glorieux, C.; Nockemann, P.; Thijs, B.; Binnemans, K.; Longuemart, S. *J. Chem. Phys.* **2008**, *128*, 064509.
(28) Ueno, K.; Tokuda, H.; Watanabe, M. *Phys. Chem. Chem. Phys.* **2010**, *12*, 1649–1658.
(29) Yoshizawa, M.; Xu, W.; Angell, C. A. *J. Am. Chem. Soc.* **2003**, *125*, 15411–15419.
(30) Belieres, J.-P.; Angell, C. A. *J. Phys. Chem. B* **2007**, *111*, 4926–4937.
(31) Greaves, T. L.; Drummond, C. J. *Chem. Rev.* **2008**, *108*, 206–237.
(32) Tokuda, H.; Hayamizu, K.; Ishii, K.; Susan, M. A. B. H. J.; Watanabe, M. *J. Phys. Chem. B* **2004**, *108*, 16593–16600.
(33) The pK_a values of Brønsted acids were taken from(a) Covington, A. K.; Davison, W. In *CRC Handbook of Chemistry and Physics*, 75th ed.; Lide, D. R., Ed.; Chemical Rubber Co. Press: Boston, MA, 1994; pp 8−43. (b) *Lange's Handbook of Chemistry*, 13th ed.; Dean, J. A., Ed.; McGraw-Hill, Inc.: New York, 1985; pp 5−18. (c) Gutowski, K. E.; Dixon, D. A. *J. Phys. Chem. A* **2006**, *110*, 12044–12054.
(34) Okazaki, H.; Soeda, M. *Applied Catalysis* **1988**, *41*, 99–108.
(35) Vogel, H. *Phys. Z.* **1921**, *22*, 645–646.
(36) Fulcher, G. S. *J. Am. Ceram. Soc.* **1923**, *8*, 339–355.
(37) Tamman, G.; Hesse, W. *Z. Anorg. Allg. Chem.* **1926**, *156*, 245–257.
(38) Böhmer, R.; Ngai, K. L.; Angell, C. A.; Plazek, D. J. *J. Chem. Phys.* **1993**, *99*, 4201–4209.
(39) Shamim, N.; McKenna, G. B. *J. Phys. Chem. B* **2010**, *114*, 15742–15752.
(40) MacFarlane, D. R.; Forsyth, M.; Izgorodina, E. I.; Abbott, A. P.; Annat, G.; Fraser, K. *Phys. Chem. Chem. Phys.* **2009**, *11*, 4962–4967.
(41) Tokuda, H.; Tsuzuki, S.; Susan, M. A. B. H.; Hayamizu, K.; Watanabe, M. *J. Phys. Chem. B* **2006**, *110*, 19593–19600.
(42) Kanzaki, R.; Uchida, K.; Hara, S.; Umebayashi, Y.; Ishiguro, S.; Nomura, S. *Chem. Lett.* **2007**, *36*, 684–685.
(43) Bartosik, J.; Mudring, A.-V. *Phys. Chem. Chem. Phys.* **2010**, *12*, 4005–4011.
(44) Anouti, M.; Caillon-Caravanier, M.; Dridi, Y.; Galiano, H.; Lemordant, D. *J. Phys. Chem. B* **2008**, *112*, 13335–13343.
(45) van Grotthuss, C. J. D. *Ann. Chim.* **1806**, *58*, 54–73.
(46) Moura Ramos, J. J.; Afonso, C. A. M.; Branco, L. C. *J. Therm. Anal. Calorim.* **2003**, *71*, 659–666.
(47) Moynihan, C. T.; Lee, S.-K.; Tatsumisago, M.; Minami, T. *Thermochim. Acta* **1996**, *280/281*, 153–162.
(48) Lopes, J. N. A. C.; Pádua, A. A. H. *J. Phys. Chem. B* **2006**, *110*, 3330–3335.
(49) Triolo, A.; Russina, O.; Bleif, H.-J.; Cola, E. D. *J. Phys. Chem. B.* **2007**, *111*, 4641–4644.
(50) Wyart, M. *Phys. Rev. Lett.* **2009**, *104*, 095901.
(51) Kapko, V.; Matyushov, D. V.; Angell, C. A. Potential-Tuning Molecular Dynamics Studies of Fusion, and the Question of Ideal Glassformers: (I) The Gay-Berne Model; arXiv:1011.2810v3 [cond-mat.soft].